Solution Structures in SDS Micelles and Functional Activity at the Bullfrog Substance P Receptor of Ranatachykinin Peptides†

Shane A. Perrine,‡ Tracy L. Whitehead,§ Rickey P. Hicks,§ John L. Szarek,‡ James E. Krause,▽ and Mark A. Simmons*,‡

Department of Pharmacology, Marshall University School of Medicine and Huntington VA Medical Center, 1542 Spring Valley Drive, Huntington, West Virginia 25704, Department of Chemistry, Mailstop 9573, Mississippi State University, Mississippi State, Mississippi 39762, and Department of Biochemistry and Molecular Biology, Neurogen Corporation, Bradford, Connecticut 06405

Received February 29, 2000

A set of novel tachykinin-like peptides has been isolated from bullfrog brain and gut. These compounds, ranatachykinin A (RTKA), ranatachykinin B (RTKB), and ranatachykinin C (RTKC), were named for their source, *Rana catesbeiana*, and their homology to the tachykinin peptide family. We present the first report of the micelle-bound structures and pharmacological actions of the RTKs. Generation of three-dimensional structures of the RTKs in a membrane-model environment using ^{1}H NMR chemical shift assignments, two-dimensional NMR techniques, and molecular dynamics and simulated annealing procedures allowed for the determination of possible prebinding ligand conformations. RTKA, RTKB, and RTKC were determined to be helical from the midregion to the C-terminus (residues 4−10), with a large degree of flexibility in the N-terminus and minor dynamic fraying at the end of the C-terminus. The pharmacological effects of the RTKs were studied by measuring the elevation of intracellular Ca^{2+} in Chinese hamster ovarian cells stably transfected with the bullfrog substance P receptor (bfSPR). All of the RTKs tested elicited Ca^{2+} elevations with a rank order of maximal effect of RTKA ≥ SP > RTKC ≥ RTKB. A high concentration (1 μM) of the neuropeptides produced varying degrees of desensitization to a subsequent challenge with the same or different peptide, while a low concentration (1 pM) produced sensitization at the bfSPR. Our data suggest differences in amino acid side chains and their charged states at the C-terminal sequence or differences in secondary structure at the N-terminus, which do not overlap according to the findings in this paper, may explain the differing degree and type of receptor activation seen at the bfSPR.

Introduction

The tachykinins are a group of neuropeptides, named for their ability to rapidly increase the contraction of smooth muscle. The primary classification of the tachykinins is based upon the shared features at the conserved carboxyl terminal sequence of the tachykinins, -Phe-Xaa-Gly-Leu-Met-NH_2, where Xaa is a variable amino acid residue.[1] The subfamily classification is based upon differences in the amino acid sequence, particularly the Xaa residue but also the amino terminal residues. The subfamilies are SP, physalaemin, eledoisin, and kassinin. The most famous and well studied of the tachykinins is SP. SP was originally isolated from the mammalian gastrointestinal tract in 1931;[2] however, its amino acid sequence was not revealed until 1970.[3] To date, over 40 different tachykinins have been isolated from a variety of species.[1,4] The tachykinins have been localized to a variety of sites in the central and peripheral nervous systems. There is evidence to support a functional role for tachykinins in control of smooth muscle tone, respiratory and cardiovascular control, nociception, inflammation, allergic reactions, and glandular secretions.[5] Tachykinins or tachykinin-like immunoreactivity has also been observed in invertebrates and in nonmammalian vertebrates, particularly in amphibians.

	1	2	3	4	5	6	7	8	9	10	11
SP	Arg	Pro	Lys	Pro	Gln	Gln	Phe	Phe	Gly	Leu	Met-NH_2
RTKA	Lys	Pro	Ser	Pro	Asp	Arg	Phe	Tyr	Gly	Leu	Met-NH_2
RTKB		Tyr	Lys	Ser	Asp	Ser	Phe	Tyr	Gly	Leu	Met-NH_2
RTKC		His	Asn	Pro	Ala	Ser	Phe	Ile	Gly	Leu	Met-NH_2

Figure 1. Amino acid sequence of the tachykinins: sequences of substance P, ranatachykinin A, ranatachykinin B, and ranatachykinin C. Note the conserved carboxyl terminus characteristic of the tachykinin family present in SP, RTKA, RTKB, and RTKC.

Four novel tachykinins have recently been isolated from brain and intestine of the bullfrog, *Rana catesbeiana*.[6] These neuropeptides have been named RTKA, RTKB, RTKC, and RTKD. The amino acid sequences of the RTKs and SP are shown in Figure 1. Three of the compounds, RTKA, RTKB, and RTKC, share the

† Abbreviations: SP, substance P; RTK, ranatachykinin; RTKA, ranatachykinin A; RTKB, ranatachykinin B; RTKC, ranatachykinin C; RTKD, ranatachykinin D; bfSPR, bullfrog substance P receptor; SDS, sodium dodecyl sulfate; 2D, two-dimensional; NMR, nuclear magnetic resonance; WATERGATE, water suppression by gradient-tailored excitation; TOCSY, total correlated spectroscopy; NOESY, nuclear Overhauser enhancement spectroscopy; NOE, nuclear Overhauser effect; RMSD, root-mean-square deviation.

* To whom correspondence should be addressed: (304)-696-7332; simmons@marshall.edu.

‡ Marshall University School of Medicine.

§ Mississippi State University.

▽ Neurogen Corporation.

10.1021/jm000093v CCC: $19.00
Published on Web 04/14/2000

conserved carboxyl terminus, which is indicative of the tachykinin family. RTKD varies due to the substitution of Gly by Ala and Leu by Pro at the 9 and 10 positions, respectively. This may suggest that RTKD does not belong to the family of tachykinins; however, it does exhibit tachykinin-like activity in guinea pig ileum and rat duodenum.[6] The only biological activity of the RTKs that has been examined to date is the relative potency for contraction of intestinal smooth muscle.[6] Neither details in the pharmacological activity of the RTKs nor their biologically active conformations have been reported.

In an ideal structure determination study, one would attempt to determine the biologically active conformation of a peptide by observing the peptide bound to its native receptor. However, the tachykinin receptors are membrane-embedded G-protein coupled receptors of large molecular weight which are very difficult to crystallize.[7] Therefore, the direct investigation of the receptor-bound conformation of these peptides is extremely limited. An additional problem in this structural investigation is that the presence of the membrane is required to maintain the biologically active conformation of the receptors.[8] The resulting size of such a peptide-receptor-membrane complex excludes structural analysis via solution NMR techniques.[8]

In an attempt to obtain structural information indirectly, neuropeptides have been investigated in the presence of a variety of membrane model systems. In earlier studies, our group has employed membrane model systems to induce stable secondary structures onto the polypeptide backbone of neuropeptides. These studies have provided a great deal of insight into the conformational basis of biological activity.[9−13] SDS micelles provide reasonable line widths and have been used extensively as a simple membrane model in NMR investigations.[14] The results of the studies showed that many neuropeptides adopt similar structures when bound to SDS micelles as to those observed in the presence of phospholipids.[15−17] On the basis of these results, it seems reasonable that SDS micelles should impart upon the RTK peptides structures which can be related to their biological activity. ^{1}H NMR chemical shift assignments for RTKA, RTKB, and RTKC were determined at 600 MHz in sodium dodecyl sulfate (SDS) micelles.

The molecular structure of the bfSPR utilized in this study was previously determined from a cDNA isolated from bullfrog sympathetic ganglion cDNA library.[18] Like its counterparts, the deduced amino acid sequence of this receptor is consistent with the seven transmembrane domain structure postulated for the family of G protein coupled receptors and shows substantial homology to the mammalian tachykinin receptors. In this study the ability of SP, RTKA, RTKB, and RTKC to increase intracellular Ca^{2+} and cause receptor desensitization in Chinese hamster ovary cells (CHO cells) stably transfected with the bfSPR was also studied. Together with the structural studies, the results of these experiments were correlated to the chemical conformation of the RTKs.

Results

I. Structural Data. Spectral Assignment. Chemical Shift Assignments. The use of two-dimensional NMR and simulated annealing methods for the determination of solution structures adopted by neuropeptides in the presence of membrane model systems is well documented in the literature.[14,19,20,21−23] ^{1}H resonance assignments were determined using the standard two-dimensional NMR sequence-specific resonance assignment techniques of Wüthrich.[56] A TOCSY[57] experiment was used in each case to identify individual amino acid spin systems by the characteristic coupling patterns of side chains. NOESY[26] experiments were then used to sequence the spin systems by following the characteristic $C^{\alpha}H-NH$ connectivity pathways. The chemical shift assignments determined for all three peptides are given in Table 1. Representative NOESY spectra showing the NH−alkyl (200 ms) and the NH to $^{\alpha}$H as well as the NH−NH sequential assignments for RTKC are given in Figure 2. Figure 3 shows the NH to H and the NH−NH *i* to *i* +2, and, *i* to *i* +3, connectivity observed in the 500 ms NOESY. NOESY spectra of the same regions of RTKA and RTKB are available in the Supporting Information.

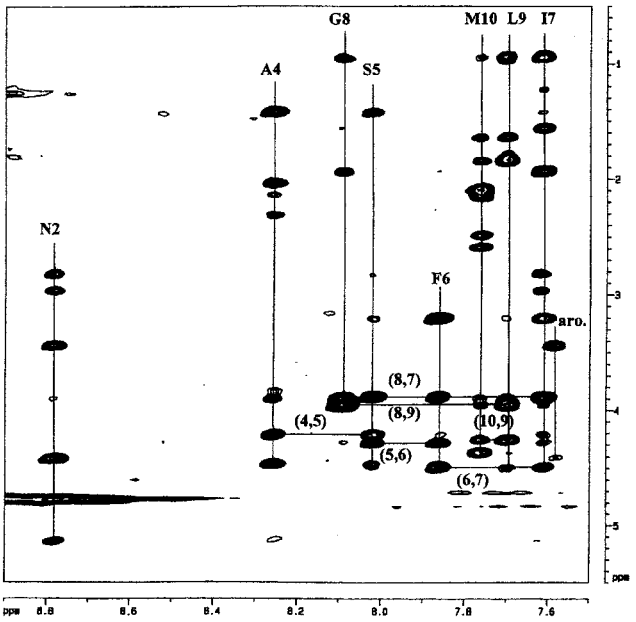

Figure 2. NH−alkyl region of the 600 MHz NOESY (200 ms mixing time) spectra for RTKC in 100 mM SDS-d_{25} micelles, 90% H_2O/10% ^2H_2O at pH = 4.0 and at 298 K.

(A) RTKA in SDS-d_{25} Micelles. All amide resonances in the TOCSY spectrum of RTKA were unique (with the exception of proline) with minimal overlap of the resonances (with the exception of the Tyr[8] and Leu[10] amide protons). Therefore, spin-system assignment was relatively straightforward. It is a common practice in our laboratory to obtain a series of variable temperature (290, 298, 303, 308 K) 1D-proton spectra of the neuropeptide to determine which temperature yields the best resolution of the amide protons (in this case, 298 K). The spin system of each amino acid residue was assigned using the method sequence-specific resonance assignment developed by Wüthrich,[24] using TOSCY[25] and NOESY[26] (200 and 500 ms mixing time) spectra.

(B) RTKB in SDS-d_{25} Micelles. Using the same method, assignments were made for RTKB. The TOSCY spectrum of RTKB exhibited spectral overlap for the following amino acid amide protons pairs: Lys[2]/Asp[4]

Table 1. ^{1}H Chemical Shifts for RTKA, RTKB, and RTKC

residue	NH	CαH	Cβ H	others
		Ranatachykinin A		
Lys-1	-	4.79	1.99	1.60 (Cγ H)
				1.79 (Cδ H)
				3.11 (Cε H
Pro-2	N/A	4.65	1.88, 2.43	2.02, 2.08 (Cγ H)
				3.56, 3.91 (Cδ H)
Ser-3	8.23	4.94	3.91	
Pro-4	N/A	4.54	2.14, 2.23	2.00 (Cγ H)
				3.77, 3.94 (Cδ H)
Asp-5	8.29	4.34	2.86	
Arg-6	8.10	4.15	1.31, 1.37	1.56, 1.74 (Cγ H)
				3.07 (Cδ H)
				7.05 (NH)
Phe-7	7.82	4.55	3.01, 3.28	7.20 (2,6H)
				7.20 (3,5H)
				7.27 (4H)
Tyr-8	7.71	4.42	3.06, 3.14	6.95 (2,6H)
				7.25 (3,5H)
Gly-9	8.19	3.86, 3.97		
Leu-10	7.73	4.27	1.82, 1.88	1.64 (Cγ H)
				0.95, 1.02 (Cδ H)
Met-11	7.75	4.44	2.04, 2.16	2.47, 2.59 (Cγ H)
				2.02 (Cδ H)
term. NH_2	6.86, 7.15			
		Ranatachykinin B		
Tyr-1	-	4.33	3.16, 3.18	7.25 (2,6H)
				6.96 (3,5H)
Lys-2	8.36	4.28	1.80	1.34 (Cγ H)
				1.69 (Cδ H)
				3.03 (Cε H)
Ser-3	8.13	4.42	3.87, 3.98	
Asp-4	8.36	4.72	2.88	
Ser-5	8.10	4.39	3.77	
Phe-6	8.11	4.47	3.08	7.17 (2,6H)
				7.23 (3,5H)
				7.26 (4H)
Tyr-7	7.80	4.29	2.97, 3.07	7.18 (3,5H)
				6.94 (2,4H)
Gly-8	7.93	3.95, 3.82		
Leu-9	7.81	4.43	1.78, 1.85	1.61 (Cγ H)
				0.96 (Cδ H)
Met-10	7.82	4.44	2.03, 2.13	2.47, 2.58 (Cγ H)
				2.00 (Cδ H)
term. NH_2	6.84, 7.08			
		Ranatachykinin C		
His-1	-	4.42	3.43, 3.90	7.58 (2H)
				6.90 (4H)
Asn-2	8.78	5.19	2.97, 2.83	6.90, 7.61 (γ NH_2)
Pro-3	N/A	4.47	2.03, 2.31	2.13 (Cγ H)
				3.21 (Cδ H)
Ala-4	8.25	4.22	1.41	
Ser-5	8.01	4.29	3.89	
Phe-6	7.86	4.49	3.21	7.28 (2,6H)
				7.25 (2,5H)
				7.23 (4H)
Ile-7	7.60	3.90	1.93	1.23, 1.56 (γ CH_2)
				0.93 (γ CH_3)
				N/A (Cδ H)
Gly-8	8.09	3.97		
Leu-9	7.69	4.26	1.84	1.63 (γ H)
				0.92 (Cδ H)
Met-10	7.75	4.37	2.09, 2.14	2.60, 2.48 (Cγ H)
				2.13 (Cε H)
term. NH_2	7.25, 6.95			

and Leu^9/Met^{10}. Similar spin systems were distinguished from one another based upon the CαH−NH connectivity pathways in the 200 ms NOESY spectrum.

(C) RTKC in SDS-d_{25} Micelles. Assignment was done as in the previous two cases. All spin systems in RTKC are unique, and overlap was nonexistent. Verification of the assignments was made by identifying the sequential connectivity pathway linking the CαH−NH resonances using the 200 ms NOESY spectrum.

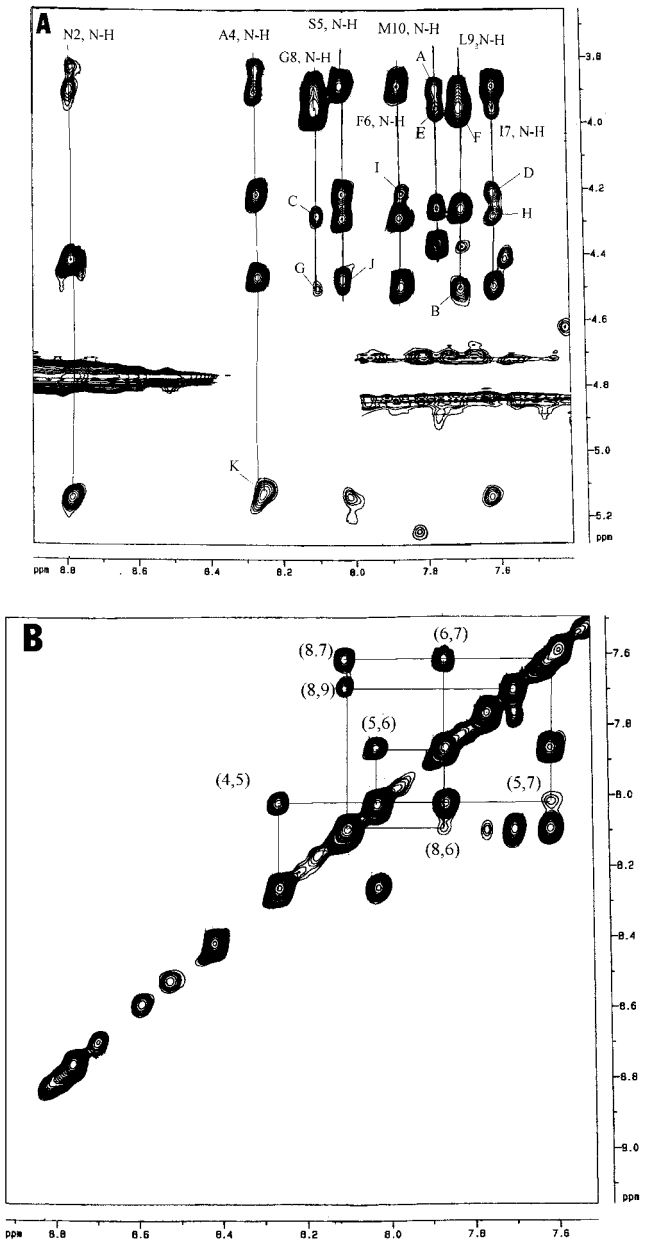

Figure 3. (A) The i to $i + 2$ and i to $i + 3$, NH−H connectivities observed in the 500 ms NOESY spectrum of RTKC. The NH−H interactions are as follows: (**A**) Met^{10} N−H to Ile^7 αH; (**B**) Leu^9 NH−Phe^6 αH; (**C**) Gly^8 N−H to Ser^5 αH; (**D**) Ile^7 N−H to Ala^4 αH; (**E**) Met^{10} N−H to Gly^8 αH; (**F**) Leu^9 N−H to Ile^7 αH; (**G**) Gly^8 N−H to Phe^6 αH; (**H**) Ile^7 N−H to Ser^5 αH; (**I**) Phe^6 N−H to Ala^4 αH; (**J**) Ser^5 N−H to Pro^3 αH; (**K**) Ala^4 N−H to Asn^2 αH. (B) The N−H to N−H region of the 500 ms NOESY spectrum of RKTC showing the i to $i + 1$, and i to $i + 2$ amide interactions.

Molecular Dynamics and Simulated Annealing. Three-Dimensional Structure. Data from three NOESY spectra were collected with mixing times of 100, 200, and 500 ms. These mixing times were selected based on our previous studies with SDS micelle-bound tachykinins. This was done for each sample in order to classify peak intensities over a range of strong to very weak corresponding to the upper-bound interproton distances of 2.7, 3.3, 4.0, and 5.0 Å.[14,20] NOEs, which first appeared in the 100 ms NOESY spectra, were assigned an upper limit value of 2.7 Å. NOEs which first appeared in the 200 ms NOESY spectrum were assigned

Table 2. Experimental and NOEs Used as Restraints in SA Calculations

compd	intra-residual	i to $i+1$	i to $i+2$	i to $i+3$	total
RTKA	20	14	6	7	47
RTKB	23	29	11	7	70
RTKC	23	31	7	2	63

Table 3. Statistical Data for RTKA, RTKB, and RTKC

compd	residues	RMSD (Å)	avg RMSD (Å)	avg energy (kcal)	violations (Å)
RTKA	4−10	0.10−0.92	0.64 ± 0.30	152.17 ± 23.22	≤0.100
RTKB	4−9	0.11−0.86	0.36 ± 0.23	216.73 ± 13.77	≤0.100
RTKC	4−9	0.15−1.13	0.56 ± 0.29	146.91 ± 7.61	≤0.100

an upper limit of 3.3 Å. NOEs which first appeared in the 500 ms NOESY spectrum were assigned upper limits of 4.0 and 5.0 Å depending on intensity. Using the distance restraints derived from the NOEs shown in Table 2, three-dimensional structures were generated for the three peptides using a molecular dynamics and simulated annealing protocol[14,20] (a complete listing of the molecular dynamics and simulated annealing protocol is given in the Supporting Information). A summary of the intraresidue as well as sequential interresidue and medium-range NOEs used as restraints for all three peptides are given in Figure 4. In all cases, 50 structures were generated, with the 25 of lowest energy being used in structural analysis. Statistical data concerning regions of global folding, RMSD values for superimposition (for all backbone atoms of the specified amino acid sequence), average energies, and distance violations for all three peptides are given in Table 3. Stereoview representations for the three peptides showing backbone superimposition are given in Figure 5.

(A) RTKA in SDS-d_{25} Micelles. The presence of a continuous run of strong NH−NH_{i+1} and medium $C^{\alpha}H-NH_{i+1}$ connectivities, along with overlapping $C^{\alpha}H-NH_{i+2}$ and $C^{\alpha}H-NH_{i+3}$ connectivities, is sufficient to suggest that a helical structure exists between residues 4−10.[24] In addition, overlapping medium $C^{\alpha}H-C^{\alpha}H_{i+3}$ connectivities between residues 4−9 support the helical structure over this region.[24]

(B) RTKB in SDS-d_{25} Micelles. A series of strong NH−NH_{i+1} and weak $C^{\alpha}H-NH_{i+1}$ connectivities, along with several overlapping NH−NH_{i+2} and $C^{\alpha}H-NH_{i+2}$ connectivities of weak intensity, suggests that a helical structure should be present between residues 2−10.[24] The helical structure is confirmed by the presence of weak $C^{\alpha}H-C^{\alpha}H_{i+3}$ connectivities between residues 3−9 and overlapping weak $C^{\alpha}H-NH_{i+3}$ connectivities between residues 4−9.[24]

(C) RTKC in SDS-d_{25} Micelles. The presence of a continuous sequence of strong NH−NH_{i+1} and weak $C^{\alpha}H-NH_{i+1}$ connectivities between residues 4−10 along with overlapping weak $C^{\alpha}H-NH_{i+2}$ connectivities is suggestive of a helical structure in this region.[24] A weak $C^{\alpha}H-C^{\alpha}H_{i+3}$ connectivity between residues 3−6 indicates the presence of a helix in this region, while overlapping weak $C^{\alpha}H-NH_{i+3}$ connectivities between residues 2−10 further indicate a helical structure for the peptide.[24]

Secondary Structure. The presence and location of peptide secondary structure was estimated using one

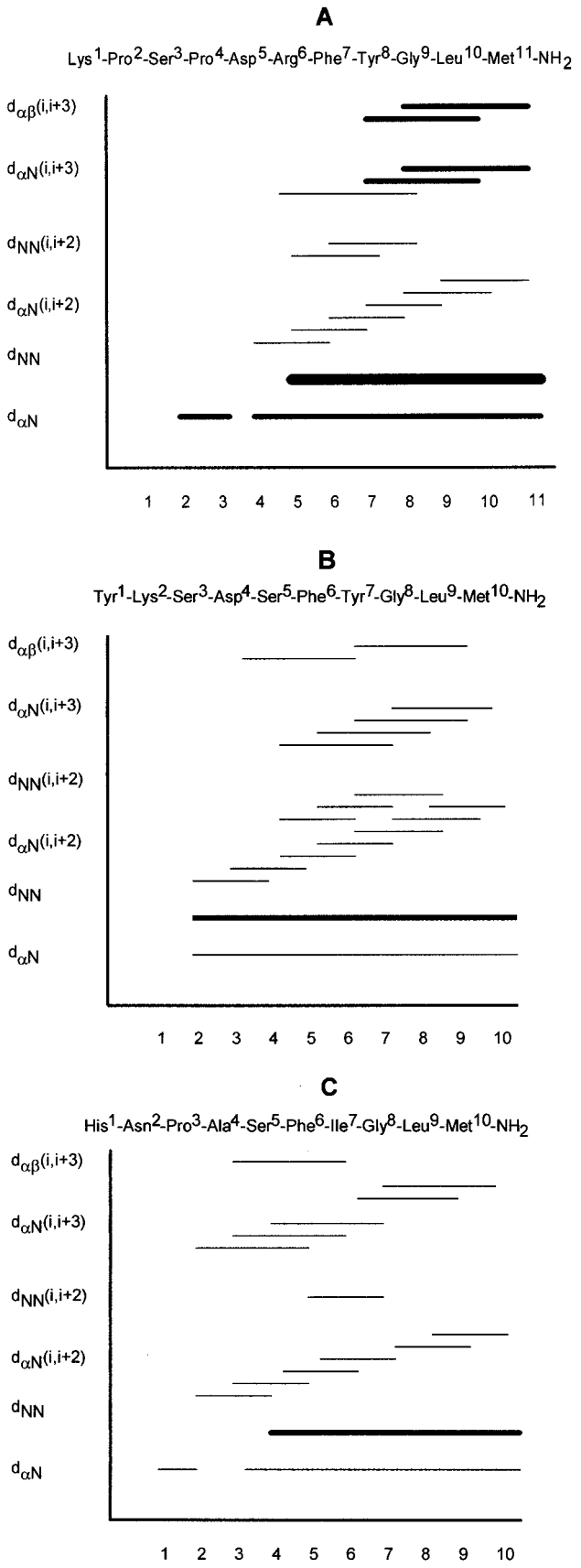

Figure 4. Summary of the sequential and medium-range NOE connectivities observed in (A) RTKA in SDS-d_{25} micelles, (B) RTKB in SDS-d_{25} micelles, and (C) RTKC in SDS-d_{25} micelles. Relative NOE intensities are represented by bar thickness.

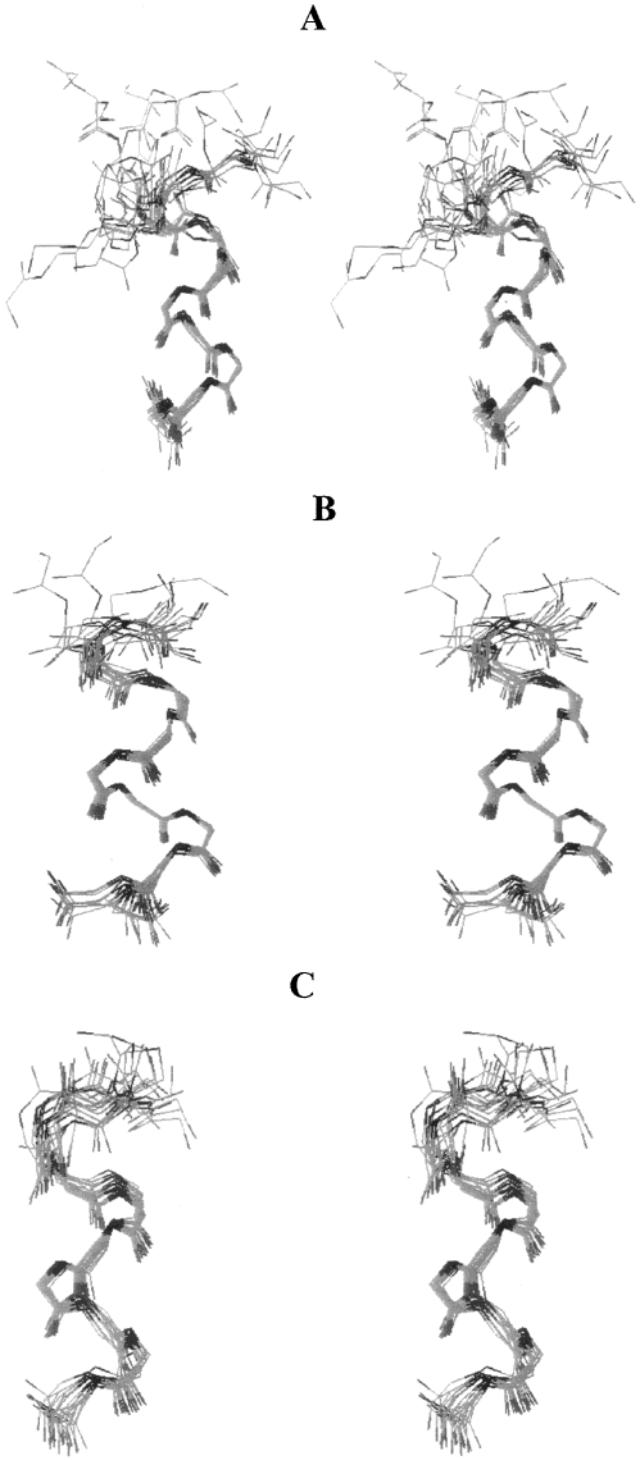

Figure 5. Stereoview superimpose of the backbone atoms of 25 refined structures of (A) RTKA in SDS-d_{25} micelles, (B) RTKB in SDS-d_{25} micelles, and (C) RTKC in SDS-d_{25} micelles [A = top, B = middle, C = bottom].

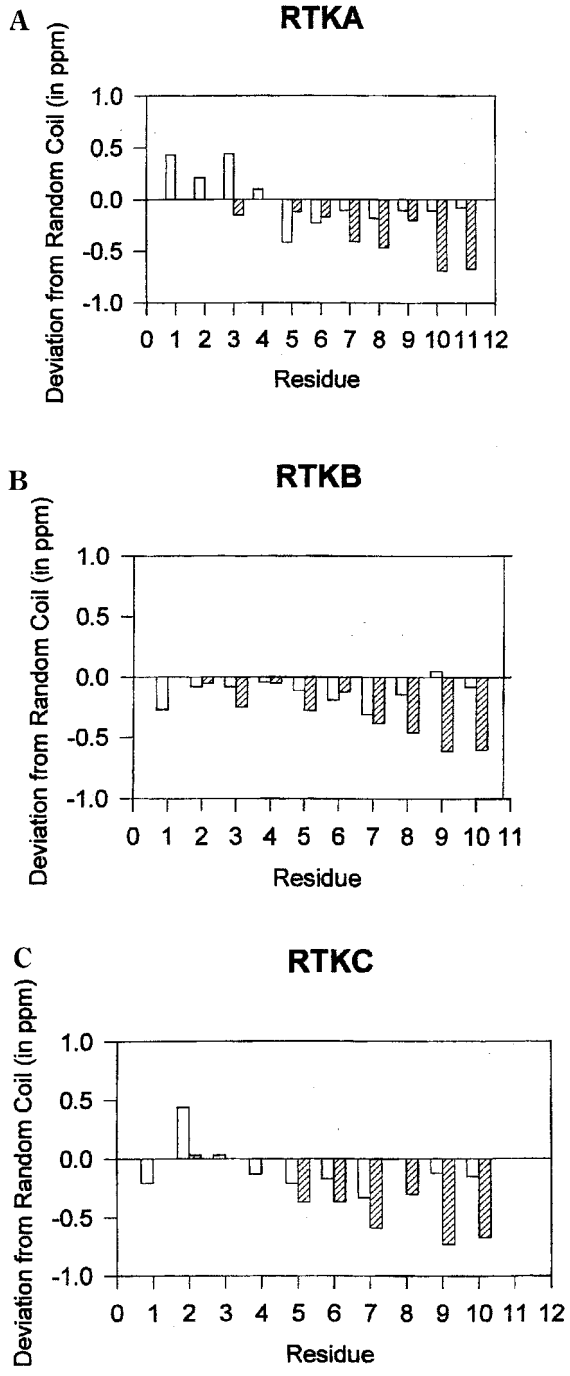

Figure 6. CSI analysis for (A) RTKA in SDS-d_{25} micelles, (B) RTKB in SDS-d_{25} micelles, and (C) RTKC in SDS-d_{25} micelles.

portion of the Chemical Shift Index (CSI) method of Wishart.[27] This method estimates certain secondary structure characteristics based on the comparative deviation of the chemical shifts of the $C^{\alpha}H$ from random coil values for each amino acid. Results for this technique are given in Figure 6, indicating secondary structures that are consistent with the NOE data. Stereoviews of the superimposition of the backbone atoms of (1) RTKA in SDS-d_{25} micelles (residues 4−9) [purple], (2) RTKB in SDS-d_{25} micelles (residues 4−8) [green], and (3) RTKC in SDS-d_{25} micelles (residues 4−8) [orange] are given in Figure 7.

II. Functional Data. Dose Response Curves for Tachykinin-Induced Ca^{2+} Transients. A typical tracing showing the Ca^{2+} change in a population of bfSPR transfected CHO cells is shown in Figure 8. This figure also illustrates the protocol used to measure desensitization. Upon application of SP (1 μM), a rapid increase in intracellular Ca^{2+} was observed (tracing 1). The Ca^{2+} level promptly returned to baseline levels. The cells were incubated for 5 min in this concentration of SP. Following a wash cells were challenged with a second application of SP (1μM) (tracing 2). Desensitiza-

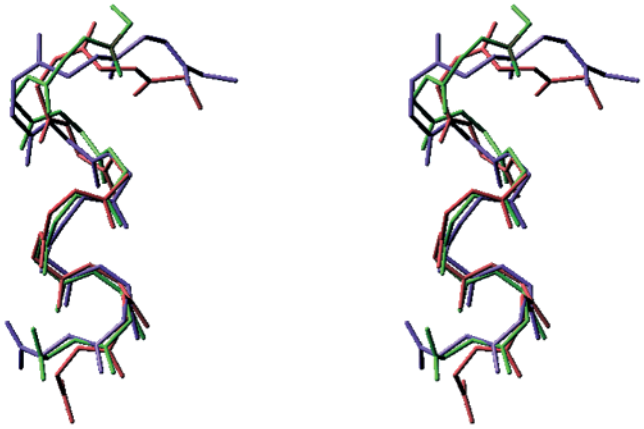

Figure 7. Stereoview of the superimposition of the backbone atoms of (1) RTKA in SDS-d_{25} micelles (residues 4−9) [purple], (2) RTKB in SDS-d_{25} micelles (residues 4−8) [green], and (3) RTKC in SDS-d_{25} micelles (residues 4−8) [orange]. The RMSD for the backbone superimposition of RTKB onto RTKA is 0.62 Å, and the RMSD for the backbone superimposition of RTKC onto RTKA is 0.49 Å.

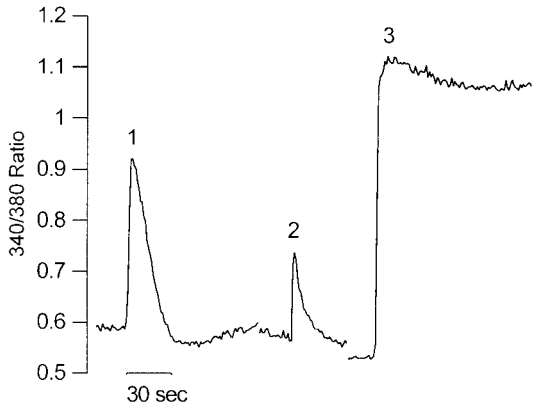

Figure 8. Typical tracing of Ca^{2+} elevations in CHO cells recorded as the ratio of 340/380 nm signal. Response after administration of first drug. Peak of Ca^{2+} elevation was used to construct dose−response curves. This application also served as a desensitizing dose for the test dose. Response after administration of test dose. Peak Ca^{2+} elevation of this response was used to construct dose−response curves for desensitization. Response elicited by ionomycin to obtain maximum Ca^{2+} elevation for each coverslip.

tion is observed as a decrease in the peak of this second response. Following another washout, the Ca^{2+} ionophore, ionomycin, was applied to determine the maximal response for that coverslip. To obtain the dose−response curve for SP, the concentration of the first application was varied.

The dose−response curve for SP is shown in Figure 9. The greatest rise in Ca^{2+} was produced by 10 nM SP, which produced an average effect equal to 49.8 ± 1% of the ionomycin response. Dose−response curves for RTKA, RTKB, and RTKC were obtained in the same manner and are also shown in Figure 9. All of the RTKs tested acted as agonists at the bfSPR to produce increases in intracellular Ca^{2+}. Similar maximal responses were obtained with each of the RTKs. EC_{50} values showed that SP and RTKA had similar potencies for the bfSPR, with values of 1 and 0.6 nM, respectively. EC_{50} values for RTKB and RTKC were 14 and 13.5 nM, respectively. In nontransfected CHO cells the tachykinins did not elicit a change in the 340/380 ratio (data not shown).

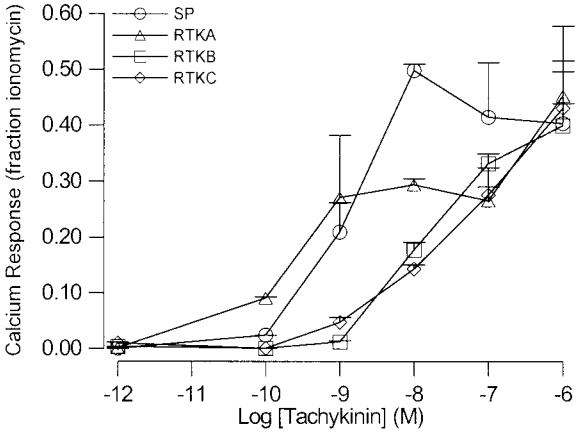

Figure 9. Dose−response curves for Ca^{2+} elevation for SP, RTKA, RTKB, and RTKC. Dose−response curves were generated by applying various concentrations of agonist and measuring the changes in Ca^{2+} elevation. Data are expressed as a fraction of the ionomycin response. Each data point represents the mean of three or more separate experiments; bars represent the standard error of the mean.

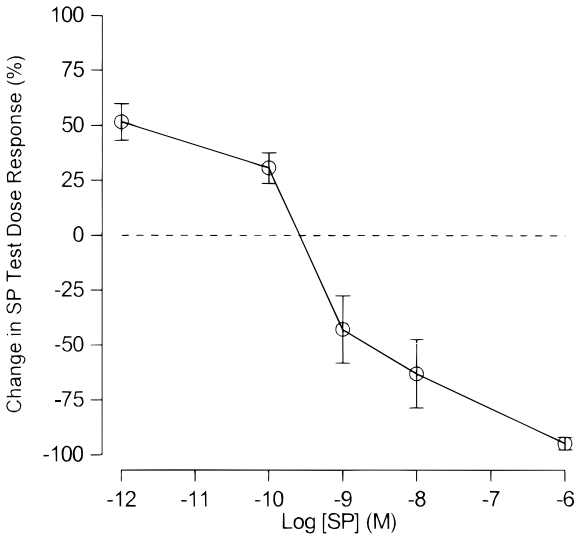

Figure 10. Dose−response curve for desensitization to SP by SP. A dose−response curve for desensitization was generated by applying various concentrations of SP for 5 min followed by application of a second fixed concentration (test dose) of 1 μM SP. Responses are shown as a percent of the response for the test dose of SP obtained in the absence of desensitization. The zero line represents no change in response to test dose. Responses below this line indicate receptor desensitization, while responses above this line indicate receptor sensitization. Each data point represents the mean of three or more separate experiments; bars represent the standard error of the mean.

SP-Induced Desensitization. Desensitization to SP was measured as the decrease in amplitude of a subsequent response to SP (1 μM) after preincubation in various concentrations of SP (Figure 8). The concentration−effect curve for desensitization to SP is shown in Figure 10. Significant desensitization ($p < 0.05$) of the response to SP was observed following pretreatment with SP greater than 1 nM, whereas significant potentiation ($p < 0.05$) of the response was seen at pretreatment doses lower than 1 nM.

Time Course of Desensitization and Resensitization for SP. The time course for desensitization to

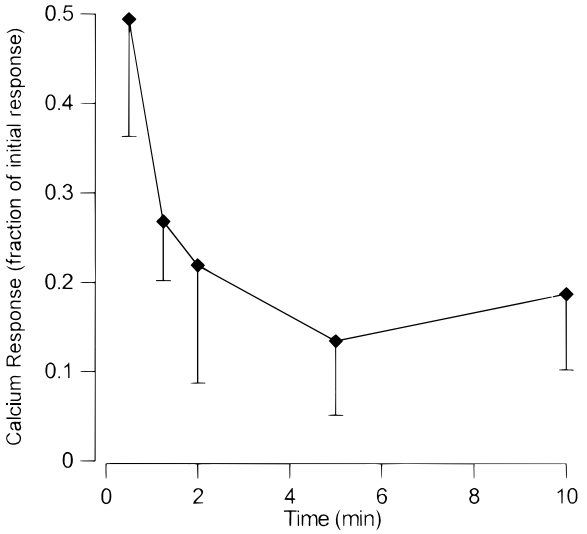

Figure 11. Time course for desensitization of SP response. An application of SP was applied with varying (0.5, 1.25, 2, 5, or 10 min) times between applications to provide desensitization. A concentration of 100 nM SP was used to provide the desensitization, followed by application of 1 μM SP to evaluate the response. Data are presented as a fraction of the initial response. Each data point represents the mean of three or more separate experiments; bars represent the standard error of the mean.

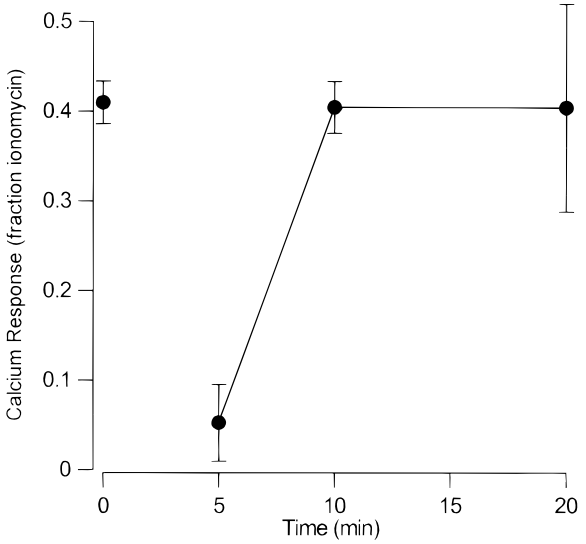

Figure 12. Time course for resensitization of SP response. An application of 1 μM SP was injected and allowed to incubate with transfected CHO cells for 2 min, washed with Ca^{2+}-containing extracellular solution, and then incubated for 2, 5, or 10 min. Following a brief washout a second application of 1 μM SP was applied, and peak intracellular Ca^{2+} elevations were recorded to evaluate the recovery of the Ca^{2+} response. The data point at time 0 min indicates the response to SP without pretreatment. Data are presented as a fraction of the ionomycin response. Each data point represents the mean of three or more separate experiments; bars represent the standard error of the mean.

SP was investigated by varying the time between the additions of the 100 nM desensitizing dose and the test dose. The results are shown in Figure 11. Following pretreatment with 100 nM SP the test response decreased to 49 ± 13% of the first dose in 30 s; near complete desensitization was seen following 5 min of incubation to 100 nM SP (13 ± 8%).

The time course for resensitization to SP was examined by first applying a dose of SP (1 μM), which results in maximal desensitization, for 2 min. Following washout and a 5, 10, or 20 min incubation without SP, SP (1 μM) was reapplied to observe the degree to which the response had recovered from desensitization, or resensitized. As seen in Figure 12, complete resensitization to SP was observed in 10 min.

Thus far, we have measured the ability of each of the tachykinins to evoke Ca^{2+} fluxes at the bfSPR, investigated the time courses for SP-induced desensitization and resensitization, and tested the ability of SP to elicit desensitization to itself. Data from the previous set of experiments have shown that all the tachykinins tested can produce Ca^{2+} transients. Thus, the effectiveness of the RTKs to produce desensitization and cross-desensitization was evaluated.

Desensitization and Cross-Desensitization of the RTKs and SP. In this series of experiments we determined the ability of SP and the RTKs to produce desensitization to themselves and also cross-desensitization to the other tachykinins. The results to these experiments are shown in Figure 13. We had expected that pretreatment, particularly with high concentrations (1 μM) of agonist, would produce desensitization to a subsequent challenge of tachykinin. Desensitization was observed in most, but not all, cases. Most interestingly, pretreatment with low concentrations (10^{-12} M) of agonist frequently resulted in an increased Ca^{2+} flux, or an apparent sensitization of the response.

Statistical analysis of Figure 13 using ANOVA showed an interaction between the desensitizing agonist and the test drug. This indicates that the effects of the desensitizing agonist are dependent upon the test drug. To determine where these differences occurred we compared the first drug curves. The first drug curves were not different when SP or RTKC were used as the test drug ($p \geq 0.069$), Figures 13a and 13d, respectively. However, there were significant differences among the first drug curves when RTKA ($p = 0.011$) and RTKB ($p < 0.001$) were used as the test drug, Figures 13b and 13c, respectively. To determine the differences among the individual first drug curves we used Student Newman Kuels post hoc test. We found that, when RTKC was used as the pretreatment drug, the effects on RTKA were greater than when the other RTKs or SP were used as the first drug ($p < 0.05$). When SP and RTKA were used as the first drugs, the effects on RTKB were similar and both greater than the effects of RTKB and RTKC as the first drug ($p < 0.05$).

When SP was the test drug (Figure 13a), preincubation with SP, RTKA, RTKB, or RTKC at a concentration of 1 μM resulted in desensitization. When the concentration of any of these agonists during the preincubation was 1 nM, the degree of desensitization was less. With a 1 pM initial concentration, no desensitization was observed for the RTKs; however, the SP test dose response was enhanced by 52% following exposure to 1 pM SP. This shows that SP cannot only produce desensitization of the bfSPR but, at low concentrations, induces sensitization. SP and RTKA produced near 100% desensitization of the initial SP challenge, while RTKB and RTKC were only able to produce 67% and 69% desensitization, respectively.

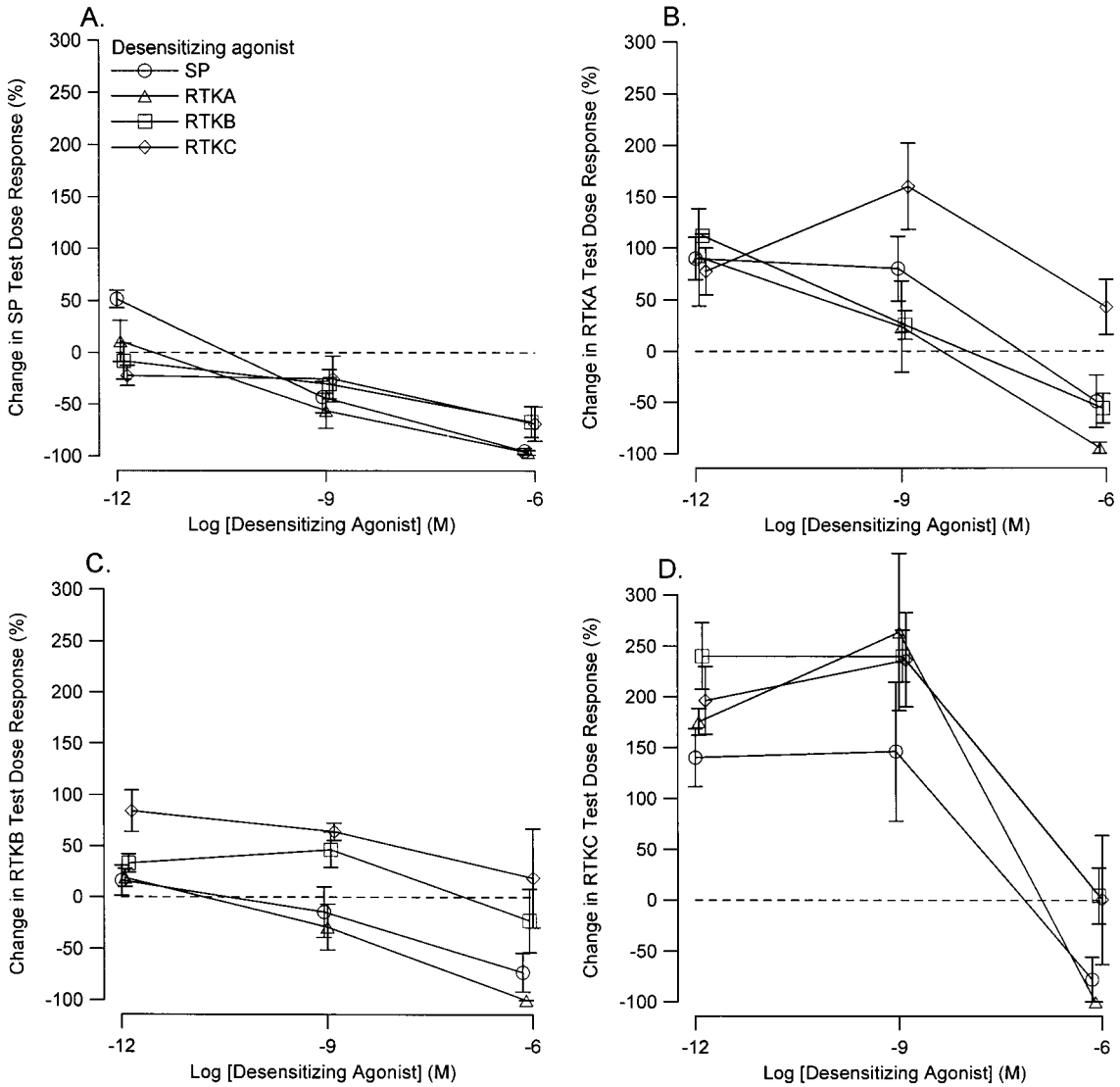

Figure 13. Dose−response curves for receptor regulation. (A) SP, (B) RTKA, (C) RTKB, and (D) RTKC as test drug. Dose−response curves for desensitization were generated by applying various concentrations of a tachykinin for 5 min followed by application of a second fixed concentration (test dose) of peptide agonist. Responses are shown as a percent of the test dose in the absence of desensitization for each tachykinin. The zero line represents no change in response to test dose. Responses below this line indicate receptor desensitization, while responses above this line indicate receptor sensitization. Each data point represents the mean of three or more separate experiments; bars represent the standard error of the mean.

Whereas only SP at a concentration of 1 pM resulted in an enhancement of the response to subsequent challenge of SP (Figure 13a), a prior incubation with either SP or any of the RTKs produced an enhancement of the RTKA response (Figure 13b). This sensitization of the RTKA response persisted when the other peptides were applied at a concentration of 1 nM. In contrast to the effects observed with SP as the test drug, desensitization of the response to RTKA was only observed following preincubation with 1 μM SP, RTKA, or RTKB (Figure 13b). RTKC failed to produce desensitization of the response to RTKA.

RTKC also failed to produce desensitization of the response to RTKB. Desensitization of the response to RTKB was only observed with high concentrations of SP and RTKA (Figure 13c). Surprisingly, RTKB, which is shown to produce desensitization of the responses to SP and RTKA, did not produce significant desensitization to itself. Potentiation of the RTKB response was observed with RTKB at 1 nM and RTKC at all tested concentrations.

The largest degree of potentiation was observed with RTKC (Figure 13d). The response to RTKC was increased 1.4 to 2.7 times control levels following pretreatment of low and moderate doses of any of the tachykinin agonists (Figure 13d). Only pretreatment with 1 μM SP and 1 μM RTKA produced desensitization of the RTKC response.

Discussion

Conformational Determinants of the RTKs. The three amphibian tachykinins in this study exhibited very similar structures to each other as well as to SP. All three were helical from the mid region to the C-terminus (residues 4−10) with a large degree of flexibility in the three N-terminal residues. On the basis of what we know about the binding of agonists to the NK_1 receptor (human and/or rat),[28−34] we can apply this

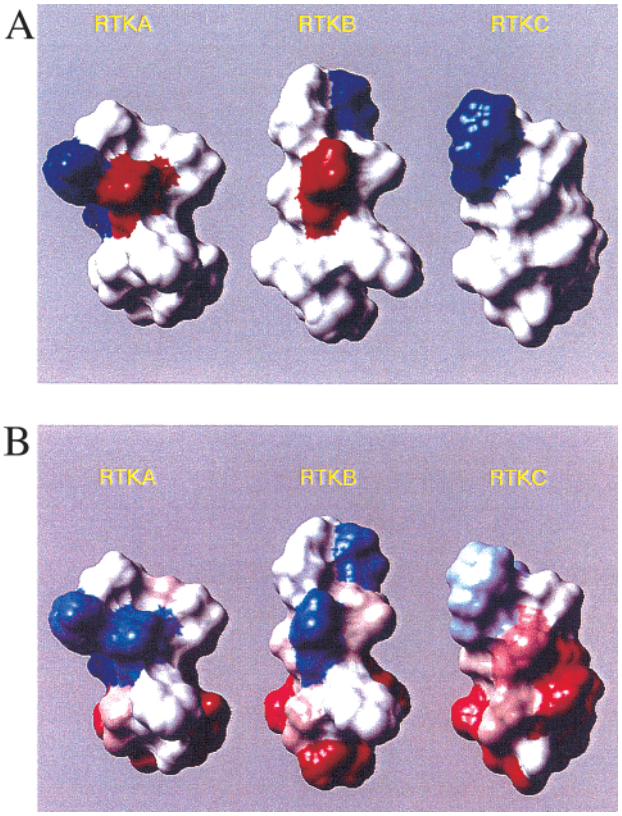

Figure 14. Figure depicting the differences in (A) charge state topography and (B) hydrophobicity for RTKA, RTKB, and RTKC. All three structures within each figure have the same relative orientation to each other to highlight major differences between the three ranatachykinins. For side chain charges, red denotes a negative residue, blue denotes a positive residue, and gray denotes a neutral residue. For hydrophobicity, increasing red denotes increasing hydrophobicity, while blue denotes increasing hydrophilicity.

information to the bullfrog SP receptor.[6,35] In a surface analysis of the averaged structures for each peptide it is seen that the hydrophobicities (Figure 14, all three peptides shown with similar orientations) of both RTKA and RTKB are very similar to each other, while that of RTKC is very different. Position eight in RTKA and position seven in RTKB are both occupied by a Tyr residue, which has a solvent accessible surface area of 229 Å^2 and a hydrophobicity value of 4.54.[36] In contrast, RTKC has an Ile residue in position seven with a solvent accessible surface area of 152 Å^2 and a hydrophobicity value of −16.71.[36] Once again, a similar size but vastly different hydrophobicity profile is seen between the two residues. It has been shown that the binding pocket for Phe^8 of SP is much larger than the binding pocket for Phe^7 of SP on the NK_1 receptor (estimated volumes of 110 and 240 Å^3, respectively).[37] Thus, it could be either the difference in hydrophobicity between Ile and Tyr or it could be the difference in size of the side chains. Due to the small size of the side chain of Ile (relative to the side chain of Tyr) fewer stabilizing intermolecular noncovalent interactions may be formed between the receptor and the Ile side chain. A reduction of "stabilizing" interactions between the receptor and the ligand will reduce the binding efficiency of the ligand.[38, 39]

It cannot be established at this time whether the structures determined in this study represent the true conformations that these three amphibian tachykinins will adopt when bound to the bfSPR. On the basis of the correlations discussed above, we feel that the conformations adopted by linear tachykinin analogues in the presence of SDS micelles provide valuable information, which can be correlated to biologically relevant structures. These structures may be the conformation that is recognized by the receptor, a conformation found at some point during the binding process, or a structure very close to the receptor-bound conformation.

Dose−Response Curves for Tachykinin-Induced Ca^{2+} Transients. The functional studies show that CHO cells transfected with the bfSPR are responsive to SP and RTKs in a dose-dependent fashion (Figure 9). The fact that the tachykinins did not increase intracellular Ca^{2+} in nontransfected CHO cells precludes the existence of an endogenous tachykinin receptor on CHO cells (data not shown).

Dose−response data also illustrate the differing abilities of the tachykinins to produce intracellular Ca^{2+} elevations. In a related study, SP-induced Ca^{2+} mobilization in CHO cells expressing the human NK_1 receptor had an EC_{50} of 0.6 nM,[40] corroborating our results using SP. Relative potencies of the ranatachykinins on guinea pig ileum were studied by Kangawa et al. upon their discovery in 1993.[5] Their results indicated a rank order of potency of SP > RTKA > RTKC > RTKB in producing smooth muscle contractions, which resembles the rank order we found in our system, RTKA ≥ SP > RTKC ≥ RTKB. Our results show that SP and RTKA are more potent than RTKB and RTKC in producing a Ca^{2+} transient. The slight difference in rank order of potencies between these studies may be a result of the receptor subtypes being expressed. In our system we are selectively expressing the bfSPR, while NK_1 and NK_3 receptors are expressed in the guinea pig ileum.[41]

Time Course of Desensitization and Resensitization for SP. Time course experiments delving into SP-induced desensitization and SP-induced resensitization clearly show that the bfSPR undergoes greater than 50% desensitization by 30 s (Figure 11) and is completely resensitized within 10 min (Figure 12) at doses providing significant desensitization. These data are consistent with other findings suggesting a rapid mechanism for desensitization. For example, using M_1-muscarinic receptors expressed in CHO cells, Waugh et al. have shown that agonist-induced desensitization is detectable within 10 s and causes loss of $Ins^{(1,4,5)}P_3$ response in a concentration-dependent manner.[42] In our system, the resensitization data shows that the receptor is fully functional and responsive in 10 min following receptor desensitization by SP (1 μM). A similar Ca^{2+} study on human NK_1 transfected CHO cells indicated a mechanism for resensitization involving receptor internalization, agonist dissociation, receptor dephosphorylation, and receptor recycling with a time course of 30 min for complete return of response following application of 100 nM SP.[43] Our results suggest that either the bfSPR resensitizes more rapidly or that resensitization of the bfSPR does not involve a time-consuming process such as receptor recycling.

Desensitization and Cross-Desensitization of the RTKs and SP. The degree and dose-dependence of cross-desensitization at the bfSPR to SP and RTKs

was examined. It was hypothesized that if the receptor had desensitized to one of the tachykinins then other tachykinin agonists with similar amino acid sequences would undergo similar degrees of receptor desensitization. However, this is not what was seen in our system. This may be due to the fact that there are distinct agonist-induced receptor conformations responsible for signal activation and desensitization. Different levels and types of receptor regulation, desensitization, and sensitization are observed depending on the concentration and agonist used. In general, we see receptor desensitization at high doses and receptor sensitization at low doses regardless of the agonist used to produce the regulation (Figure 13).

We have found that the abilities of an agonist to produce signal activation, in our case a Ca^{2+} flux, and desensitization of the response at the receptor do not strictly correlate. All agonists tested produced a receptor-dependent rise in intracellular Ca^{2+} (Figure 9); however not all agonists had the ability to cause desensitization at the bfSPR. While Ca^{2+} mobilization induced by RTKA nearly equaled that of SP, preincubation with 1 nM of any of the tachykinins produced desensitization to subsequent challenges of SP, but failed to produce desensitization to RTKA. Similarly, RTKB and RTKC both produced a Ca^{2+} influx with EC_{50} of approximately 14 nM. Despite their ability to activate the receptor and increase Ca^{2+}, RTKB and RTKC generally produced less desensitization than SP and RTKA.

An unexpected and novel finding in this study is the apparent sensitization of the Ca^{2+} mobilization following prior application of tachykinin. Like receptor desensitization, this potentiation of the response was not seen in all cases and did not correlate with the degree of signal activation for SP and the RTKs. Generally, sensitization of the response was seen at low pretreatment doses and was not observed for SP as test drug. All the tachykinins caused profound sensitization when RTKC was used as test drug. Preincubation with any tachykinin caused a 140% to 270% increase in response compared to that without pretreatment.

This wide degree and type of receptor regulation may be a result of various conformational compatibilities between the receptor and the ligand as proposed by Haung et al. based on the receptor binding properties of tachykinins.[44] This concept may be extended to include not only ligand binding properties, but other consequences of ligand−receptor interaction. Several different aspects of peptide conformation may result in the activation of more than one response through a single receptor. In our system, there are at least two different responses—signal activation and regulation of receptor sensitivity. There may be three distinct responses—activation, desensitization, and sensitization. Each of these activities may correspond to a unique conformational compatibility between ligand and receptor. This suggests that there may be different active forms of the receptor for the different activities. The molecular bases of these differences remain to be elucidated.

Structure−Activity Role of SP and the Rana-tachykinins. While the secondary structure and function of SP are known, the correlation between the amino acid sequence and biological activity of SP is not completely understood. Structural and functional studies indicate the SP molecule has two distinct regions, a C-terminal receptor binding region and an N-terminal region involved in biological regulation. It has been shown that substitution of Gly^9 by Ala or D-Gly has no effect on the pharmacological activity of SP, but substituting Phe^7, Leu^{10}, or Met^{11} decreases activity.[45,46] Josien and co-workers[37] reported that the receptor "binding pocket" for residue seven of SP is smaller in volume than the receptor "binding pocket" for residue eight. In their work, they reported that the substitution of Phe^8 of SP with Met did not effect the biological activity (binding potency) of this analogue when compared to SP.[37] Substitution of Phe^7 with Met reduced the biological activity for this analogue 4 orders of magnitude when compared to SP.[37] Replacement of Phe^8 with the conformationally restrained larger un-natural amino acid Flg (fluorenylglycine) had no effect on the biological activity of this analogue when compared to SP,[37] while replacement of Phe^7 with the same residue reduced the biological activity of this analogue by 3 orders of magnitude as compared to SP.[37]

Amino acid substitutions in the carboxy-terminal portion of the sequence have the greatest effects in altering the biological activity of the tachykinin peptides. Therefore, it is this portion of the molecule that has received the most attention in studies of the structure−activity relationships of the tachykinins. It is clear that the C-terminal pentapeptide alone contains considerable biological activity.[47] Removal of the methionineamide abolishes biological activity of SP.[48] Using chimeric NK_1 and NK_3 receptors, Tian et al. have shown that the C-terminal sequence of SP is important in determining binding affinities, while the N-terminal sequence seems to be more important in maintaining the appropriate conformation of the peptide for receptor binding and selectivity.[49]

In this study we have shown that residues 4−9 of RTKA, RTKB, and RTKC exist in a similar conformation as determined in a SDS micelle system. This findings as well as the amino acid conservation supports the hypothesis that the biological activity and receptor binding to the bfSPR are confined to the C-terminus. Since this portion of the neuropeptides is nearly conserved in primary and secondary structure, few possibilities arise to explain the degree of peptide activity at the receptor on the basis of structure alone. One explanation is that differences in amino acid side chains and their charged states at the C-terminal sequence determine the peptide's activity. Alternatively, differences at the N-terminus, which do not overlap according to the findings in this paper, may explain the differing degree and type of receptor activation. A more likely explanation is that both the side chain properties and amino acid structure affect the ability of these peptides to interact with the bfSPR.

In conclusion, the results of our study suggest that minor differences in peptide structure result in differences in pharmacological effect. Comprehension of these structure and activity relationships may allow for the development of pharmacological agents that take advantage of these properties. For example, understanding differences in ligand-induced receptor regulation may

aid in the development of drugs that do not produce desensitization or drugs that increase the effectiveness of endogenous neurotransmitters by producing an increase in receptor sensitvity.

Experimental Procedures

Sample Preparation. Samples for all three peptides (RTKA, RTKB, RTKC) were prepared using 500−700 μL aliquots of a solution composed of 1 mM peptide and 100 mM SDS-d_{25} in 90% H_2O/10% ^2H_2O. All samples were buffered using a 150 mM sodium acetate buffer to a pH of 4.0. pH's were measured using a Corning model 240 pH meter and were uncorrected for the deuterium isotope effect.

Nuclear Magnetic Resonance. ^{1}H NMR experimental data for RTKA, RTKB, and RTKC were collected using a Bruker AMX-600 spectrometer. The 2D pulse sequences used included the TOCSY with a modified MLEV-17 spin-lock sequence[50] and a 80 ms total mixing time including 2.5 ms trim pulses at both the beginning and end of the sequence, as well as NOESY[26] experiments with mixing times of 100, 200, and 500 ms. Solvent suppression was accomplished by application of the WATERGATE[51−54] (WATER suppression by GrAdient Tailor Excitation) pulse sequence developed by Sklenar and co-workers.[51] This sequence provides excellent suppression of the water resonance by a combination of rf pulses and a series of gradient pulses.[51] The sequence combines a nonselective 90 pulse with a symmetrical echo formed by two short gradient pulses in conjunction with a 180 selective (on water) pulse train.[51] Spectra for RTKA, RTKB, and RTKC in SDS-d_{25} were collected with 128 transients and 1024 t_1 increments, with 1.5 s recycle delays for all experiments. Data were collected at 298 K for all three peptides. The spectral width was 9090.9 Hz in both dimensions, and all spectra were acquired with 2048 data points in F_2. All chemical shifts were referenced internally to DSS (0.00 ppm). Spectra were processed using UXNMR (Bruker) on an ASPECT X-32 data station. Data were multiplied by a 90° shifted sine-bell window function in each dimension before transformation to produce matrixes, which consisted of 1024 data points in both dimensions. In certain applications, a trapezoidal window function, as well as 2048 × 2048 matrixes were used to enhance spectral resolution of peaks.

Estimation of Distance Constraints. Data from the three NOESY experiments conducted for each sample were used to classify peak volumes over a range of strong to very weak corresponding to the upper-bound interproton distance restraints of 2.7, 3.3, 4.0, and 5.0 Å[55,56] with strong NOEs (2.7 Å) taken from the 100 ms NOESY, medium NOEs (3.3 Å) taken from the 200 ms NOESY, and weak−very weak NOEs (4.0 and 5.0 Å) taken from the 500 ms NOESY. Since stereospecific assignments could not be made initially, pseudoatoms were employed using the center-of-mass approach, with both intraresidue and long-range correction factors added to the distance restraints. In the case of terminal methyl groups, a distance correction of 0.5 Å was added to the upper limits for distance restraints.[55] After one set of MD/SA calculations, stereospecific assignments were made by manually measuring interproton distances and selecting those that were within the acceptable distance range. Correction factors were removed and MD/SA calculations were repeated.

Molecular Dynamics and Simulated Annealing. Three-dimensional structures were generated using the experimental NOE distance restraint types shown in Table 2 using the software package DISCOVER (MSI) operating on a Silicon Graphics Iris Crimson workstation. A set of 50 structures was generated for each of the three systems by starting from templates with completely randomized backbone ϕ and ψ torsion angles and extended side chains, followed by the application of a MD/SA protocol similar to that used earlier by our group for other tachykinins as well as other neuropeptides.

Expression of bfSPR cDNA in CHO Cell Line. The bfSPR cDNAs were cloned Into the expression vector pM^{2}AH as previously described.[57] CHO cells, grown in minimal essential medium-α (α-MEM) containing 10% fetal bovine serum (FBS), were transfected with the appropriate pM^2 construct using a calcium phosphate procedure previously described.[58] After 6−10 days of selective growth in the presence of 0.8 mg/mL active Geneticin (G418), clonal colonies were isolated with a paper disk technique,[59] propagated, and screened by ligand binding.

Cell Culturing and Loading of Calcium Indicator Dye. Transfected CHO cells were maintained in α-MEM containing 10% FBS and 0.8 mg/mL G418. Cells were grown to 80 to 90% confluency on 25 mm diameter quartz cover slips and incubated at 37 °C and 5% CO_2 for 3−4 days prior to use. On the day of the experiment, coverslips were rinsed three times with Ca^{2+}-free extracellular solution (ES), containing 1 mM $MgCl_2$, 5 mM KCl, 115 mM NaCl, 10 mM HEPES, and 10 mM glucose at pH 7.4, prior to being placed in the loading chamber of a CAF-110 Intracellular Ion Analyzer (Jasco Corp., Tokyo, Japan) at 37 °C. The CAF-110 reads fluorescence from ∼3.1 mm^2 area in the center of the coverslip. The average population of cells tested in this area was ∼3000. Ca^{2+}-free ES supplemented with 5 μM Fura PE3 (AM), a calcium indicator dye, and 0.1% pluronic F-127 (Texas Fluorescence Labs, Austin, TX) was added to the chamber, and uptake of the dye was allowed to proceed for 30 min. Following loading, cells were rinsed with Ca^{2+}-free ES and incubated for 30 min in an ES containing 2.3 mM $CaCl_2$. The cells were rinsed again with Ca^{2+}-containing ES just prior to measurement of cytosolic Ca^{2+} concentrations. The ratio of fluorescence emission at 510 nm following excitation at 340 and 380 nm was used as an index of intracellular Ca^{2+} concentrations.

Dose−Response Relationships for Ca^{2+} Transients and Cross Desensitization for SP and RTKs. Dose−response curves were generated by applying various concentrations of each tachykinin (tracing 1 in Figure 8) and recording the peak of the increase in the 340/380 ratio. To examine the dose−response relationship for desensitization, cells were incubated with drug for 5 min and then washed with Ca^{2+}-containing ES. Next, a selected concentration of test drug was applied, and the change in the 340/380 ratio was recorded. The concentrations of the test drugs were SP, 1 μM; RTKA, 100 nM; RTKB, 10 μM; and RTKC, 100 nM. After recording the response, the cells were washed with Ca^{2+}-containing ES and then the peak response to ionomycin (10 μM) was recorded.

Time Course of Desensitization for SP. A time course for desensitization was obtained by applying SP and varying the incubation time between the first application and second application. SP (100 nM) was used as the desensitizing doses. SP was allowed to incubate for 0.5, 1.25, 2, 5, or 10 min after injection, and then the cells were washed with Ca^{2+}-containing ES. The second application of SP (1 μM) was then added and allowed to incubate for 1 min. Following a wash with Ca^{2+}-containing ES, 10 μM ionomycin was added and peak response recorded.

Time Course of Resensitization for SP. Resensitization of the SP response was measured by first providing adequate desensitization, then a period of resensitization, and finally measurement of the degree of resensitization. First, coverslips were allowed to incubate for 2 min in 1 μM SP; then they were washed with Ca^{2+}-containing ES. Cells were incubated for 5, 10, or 20 min. After a wash with Ca^{2+}-containing ES, a second 1 μM dose of SP was added to observe the degree to which the response had recovered. This was followed by a wash with Ca^{2+}-containing ES and recording of peak response due to the injection of ionomycin (10 μM).

Statistics. Measurements were normalized to the ionomycin response for each population of cells tested. Data are expressed either as the fraction of the ionomycin response or as a fraction of control response. Values are stated as the mean ± SEM. Statistical analysis was performed using analysis of variance (ANOVA) and Student Newman Kuels post hoc tests (SPSS version 8.0, Chicago, IL). E_{max} values were determined as the maximum response observed for each peptide and expressed as the fraction of the ionomycin response. EC_{50}

values were calculated based on nonlinear regression of the mean dose−response curves. The nonlinear equation used to fit the curves was as follows: $y = -a/[1 + (\text{concentration}/c)^b] + a$, where a = maximum response, b = slope of the curve, and $c = EC_{50}$.

Materials. Substance P and ionomycin were purchased from Sigma (St. Louis, MO). The RTKs were synthesized by the protein and nucleic acid core laboratory at Washington University in St. Louis. Deuterated sodium acetate and deuterated acetic acid were purchased from Sigma and used without further purification. Isotopically enriched ^2H_2O was purchased from ISOTEC, Inc. Perdeuterated SDS and 2,2-dimethyl-2-silapentane-5-sulfonate (DSS) were purchased from Cambridge Isotope Company. Most chemicals were purchased from Sigma or Fisher Scientific (Pittsburgh, PA).

Acknowledgment. The chemical research was supported in part by the National Institutes of Health (NIH/HSS Grant 1R15 NS 36389-01A1 [NMR facilities]), National Science Foundation (Grant CHE-92124521 [computer facilities]), National Science Foundation (Grant CHE-9205329), the State of Mississippi, and Mississippi State University to R.P.H. The pharmacological research was supported by NS25999 from the National Institute of Neurological Disorders and Stroke to M.A.S. and an ASPET 1997 Summer Undergraduate Research Fellowship to S.A.P. Some of these results were presented in abstract form at the Experimental Biology 1998 meeting in San Francisco, CA.

References

(1) Maggio, J. E.; Mantyh, P. W. History of tachykinin peptides. *The Tachykinin Receptors*; Buck, S. H., Ed.; Humana Press: Totowa, NJ, 1994.
(2) Von Euler, U. S.; Gaddum, J. H. An unidentified depressor substance in certain tissue extracts. *J. Physiol.* **1931**, *72*, 74−86.
(3) Chang, M. M.; Leeman, S. E. Isolation of a sialogogic peptide from bovine hypothalamic tissue and its characterization as substance P. *J. Biol. Chem.* **1970**, *245*, 4784−4790.
(4) Maggi, C. A. The Mammalian Tachykinin Receptors. *Gen. Pharmacol.* **1995**, *26*, 911−944.
(5) Otsuka, M.; Yoshioka, K. Neurotransmitter functions of mammalian tachykinins. *Physiol. Rev.* **1993**, *73*, 229−308.
(6) Kangawa, K.; Kozawa, H.; Hino, J.; Minamino, N.; Matsuo, H. Four novel tachykinins in frog (*Rana catesbeiana*) brain and intestine. *Regul. Pept.* **1993**, *46*, 81−88.
(7) Mantyh, P. W.; Vigna, G. R.; Maggio, J. E. Receptor Involvement in the Pathology and Disease in the Tachykinin Receptor. *The Tachykinin Receptors*; Buck, S. H., Ed.; Humana Press: Totowa, NJ, 1994.
(8) Evans, J. N. S. Biomolecular NMR Spectroscopy; Oxford University: Oxford, 1995.
(9) Ketchem, R. R.; Hu, W.; Cross, T. A. High-resolution conformation of gramicidin A in lipid bilayer by solid-state NMR. *Science* **1993**, *261*, 1457−1460.
(10) Batenburg, A. M.; Esch, J. H. v.; Kruijff, B. D. Melitin-Induced Changes of the Microscopic Structure of Phosphatidylethanolamines. *Biochemistry* **1988**, *27*, 2324−2331.
(11) Chupin, V.; Leenhouts, J. M.; de Kroon, A. I. P.; de Kruijff, B. Secondary Structure and Topology of a Mitochondrial Presequence Peptide Associated with Negatively Charged Micelles. A 2D 1H NMR Study. *Biochemistry* **1996**, *35*, 3141−3146.
(12) Young, J. K.; Hicks, R. P. Two-Dimensional NMR and Molecular Modeling Investigations of the Neuropeptide Bradykinin in three Solvent Systems: DMSO, SDS micelles and 90% Dioxane/water, Evidence for a β turn at the C-terminus in all Three Systems. *Biopolymers* **1994**, *34*, 611−623.
(13) Graham, W. H.; Carter, E. S.; Hicks, R. P. Conformational Analysis of Met-Enkephalin in Both Aqueous Solution and in the presence of Sodium Dodecyl Sulfate Micelles Using Multidimensional NMR and Molecular Modeling. *Biopolymers* **1992**, *32*, 1755−1764.
(14) Young, J. K.; Anklin, C.; Hicks, R. P. Nuclear Magnetic Resonance and Molecular Modeling Investigations of the Neuropeptide Substance P in the Presence of 15 mM Sodium Dodecyl Sulfate Micelles. *Biopolymers* **1994**, *34*, 1449−1462.
(15) Lee, S. C.; Rusell, A. F.; Laidig, W. D. Three-Dimensional structure of bradykinin in SDS micelles. *Int. J. Pept. Protein Res.* **1990**, *35*, 367−377.
(16) Zetta, L.; Marco, A. D.; Zannoni, G. Evidence for a Folded Structure of Met-Enkephalin in Membrane Mimetic Systems: 1H-nmr Studies in Sodium dodecyl sulfate, Lyso-Phosphatidylcholine and Mixed Lyso-Phophatidycholine/Sulfate Micelles. *Biopolymers* **1988**, *25*, 2315−2323.
(17) Marcinowski, K. J.; Shao, H.; Clancy, E. L.; Zagorski, M. G. Solution Structure Model of Residues 1-28 of the Amyloid β-Peptide When Bound to Micelles. *J. Am. Chem. Soc.* **1998**, *120*, 11082−11091.
(18) Simmons, M. A.; Brodbeck, R. M.; Karpitskiy, V. V.; Schneider, C. R.; Neff, D. P. A.; Krause, J. E. Molecular characterization and functional expression of a substance P receptor from the sympathetic ganglion of *Rana catesbeiana*. *Neuroscience* **1997**, *79*, 1219−1229.
(19) Wooley, G.; Deber, C. Peptides in Membranes: Lipid-induced Secondary Structure of Substance P. *Bioploymers*, **1987**, *26*, 109−121.
(20) Whitehead, T.; McNair, S.; Hadden, C.; Young, J.; Hicks, R. Membrane-Induced Secondary Structures of Neuropeptides: A Comparison of the Solution Conformations adopted by Agonists and Antagonists of the Mammalian Tachykinin NK_1 Receptor. *J. Med. Chem.* **1998**, *41*, 1497−1506.
(21) Pellegrini, M.; Mammi, S.; Peggion, E.; Mierke, D. F. Threonine^6-Bradykinin: Structural Characterization in the Presence of Micelles by Nuclear magnetic Resonance and Distance Geometry. *J. Med. Chem.* **1997**, *40*, 92−98.
(22) Malikayil, J. A.; Edwards, J. V.; Mclean, L. R. Micelle-Bound Conformations of a Bombesin/Gastrin Releasing Peptide Receptor Agonist and an Antagonists by Two-Dimensional NMR and Restrained Molecular Dynamics. *Biochemistry* **1992**, *31*, 7043−7049.
(23) Cowsik, S. M.; Lucke, C.; Ruterjans, H. Lipid-induced Conformation of Substance P. *J. Biomol. Struct. Dyn.* **1997**, *15* (1), 27−36.
(24) Wüthrich, K.; Billeter, M.; Braun, W. Polypeptide Secondary Structure Determination by Nuclear Magnetic Resonance Observation of Short Proton−Proton Distances. *J. Mol. Biol.* **1984**, *180*, 715−740.
(25) Eich, G.; Bodenhausen, G.; Ernst, R. R. Coherence Transfer by Isotropic Mixing: Application to Proton Correlation Spectroscopy. *J. Am. Chem. Soc.* **1982**, *104*, 3731.
(26) States, D. J.; Haberkorn, R. A.; Rubin, D. J. A. Two-Dimensional Nuclear Overhauser Experiment with Pure Absorption Phase in Four Quadrants. *J. Magn. Res.* **1982**, *48*, 286−292.
(27) Wishart, D.; Sykes, B.; Richards, F. The Chemical Shift Index: A Fast and Simple Method for the Assignment of Protein Secondary Structure through NMR Spectroscopy. *Biochemistry* **1992**, *31*, 1647−1651.
(28) Chassaing, G.; Convert, O.; Lavielle, S. Preferential conformation of substance P in solution. *Eur. J. Biochem.* **1986**, *154*, 77−85.
(29) Convert, O.; Duplaa, H.; Lavielle, S.; Chassaing, G. Influence of the Replacement of Amino Acids by its D-Enantiomer in the Sequence of Substance PP.2 Conformational Analysis by NMR and Energy Calculations. *Neuropeptides* **1991**, *19*, 259−270.
(30) Laoui, A. C.; Luttmann, C.; Morize, I. Pantel, G.; Morgat, A.; Rubin-Carrez, C.; Laroche, V.; Guitton, J. D.; Gigonzac, O.; James-Surcouf, E. *Molecular Mimics as Approaches for Rational Drug Design: Application to Tachykinin Antagonists*; Academic Press: London, 1995.
(31) Seelig, A.; Seelig, J. Interaction of drugs and peptides with the lipid membrane. In *Structure and Function of 7TM Receptors*. Schwartz, T. W., Hjorth, S. A., Kastrup, J. S., Eds.; Munksgaard: Copenhagen, 1996; pp 184−193.
(32) Seelig, A.; Alt, T.; Lotz, S.; Holzemann, G. Binding of Substance P Agonists to Lipid membranes and to the Neurokinin-1 Receptor. *Biochemistry* **1996**, *35*, 4365−4374.
(33) Seelig, A. Substance P and antagonist surface activity and molecular shape. *Biochem. Biophys. Acta* **1990**, *1030*, 111−118.
(34) Seelig, A. Interaction of a Substance P agonist and Substance P antagonists with lipid membranes: A thermodynamics analysis. *Biochemistry* **1992**, *31*, 2897−2904.
(35) Kozowa, H.; Hino, J.; Minamino, N.; Kanawa, K.; Matsuo, H. Isolation of four novel tachykinins from frog (*Rana catesbeiana*) brain and intestine. *Biochem. Biophys. Res. Commun.* **1991**, *177*, 588−595.
(36) Darby, N.; Creighton, T. Basic aspects of polypeptide structure. *Protein Structure*; Rickwood, D., Ed.; IRL Press: Oxford, 1993.
(37) Josien, H.; Lavielle, S.; Brunissen, A.; Saffroy, M.; Torrens, Y.; Beaujouan, J. C. Restricted Phenylalanines and their use of Structure−Activity Studies on the Tachykinin NK1 Receptors. *J. Med. Chem.* **1994**, *37*, 1586−1601.
(38) Norel, R.; Lin, L. S.; Wolfson, H. J.; Nussinov, R. Shape Complementarity at Protein−Protein Interfaces. *Biopolymers* **1994**, *34*, 933−940.
(39) Williams, D. H.; Westwell, M. S. Aspects of weak interactions. *Chem. Soc. Rev.* **1998**, *27*, 57−63.

(40) Turcatti, G.; Zoffmann, S.; Lowe, J. A., III; Drozdal, S. E.; Chassaing, G.; Schwartz, T. W.; Chollet, A. Characterization of Non-peptide antagonist and peptide agonist binding sites of the NK1 receptor with fluorescent ligands. *J. Biol. Chem*. **1997**, *272*, 21167−21175.
(41) Burcher, E.; Mussap, C. J.; Stephenson, J. A. Autoradiographic Localization of Receptors in Peripheral Tissues. *The Tachykinin Receptors*; Buck, S. H., Ed.; Humana Press: Totowa, NJ, 1994.
(42) Waugh, M. G.; Challiss, R. A. J.; Berstein, G.; Nahorski, S. R.; Tobin, A. B. Agonist-induced desensitization and phoshporylation of M1-muscarinic receptors. *Biochem. J*. **1999**, *338* (1), 175−183.
(43) Garland, A. M.; Grady, E. F.; Lovett, M.; Vigna, S. R.; Frucht, M. M.; Krause, J. E.; Bunnet, N. W. Mechanisms of desensitization and resensitization of G protein-coupled neurokinin$_1$ and neurokinin$_2$ receptors. *Mol. Pharmacol.* **1996**, *49*, 438−446.
(44) Huang, R. C.; Huang, D.; Strader, C.; Fong, T. M. Conformational compatibility as a basis of differential affinities of tachykinins for the neurokinin-1 receptor. *Biochemistry* **1995**, *34*, 16467−16472.
(45) Couture, R.; Fournier, A.; Magnan, J.; St.-Pierre, S.; Regoli, D. Structure−activity studies on substance P. *Can. J. Physiol. Pharmacol.* **1979**, *57*, 1427−1436.
(46) Duplaa, H.; Chassaing, G.; Lavielle, S.; Beaujouan, J. C.; Torrens, Y.; Saffroy, M.; Glowinski, J.; D'Orleans-Juste, P.; Regoli, D.; Carruette, A.; Garret, D. Influence of replacement of amino acid by its D-enantiomer in the sequence of substance P. 1. Binding and pharmacological data. *Neuropeptides* **1991**, *19*, 251−257.
(47) Bury, R. W.; Mashford, M. L. Biological activity of C-terminal partial sequences of substance P. *J. Med. Chem*. **1976**, *19*, 854−856.
(48) Anastasi, A.; Falconieri-Erspamer, G. Occurrence of phyllomedusin a physalaemin-like decapeptide in the skin of *Phyllomdusa bicolor*. *Experientia* **1970**, *26*, 866−867.
(49) Tian, Y.; Lan-Hsin, W.; Oxender, D. L.; Chung, F. The unpredictable high affinities of a large number of naturally occurring tachykinins for chimeric NK1/NK3 receptors suggest a role for an inhibitory domain in determining receptor specificity. *J. Biol. Chem*. **1996**, *271*, 20250−20257.
(50) Bax, A.; Davis, D. MLEV-17 Based Two-Dimensional Homonuclear Magnetization Transfer Spectroscopy. *J. Magn. Reson*. **1985**, *65*, 355−360.
(51) Sklenar, V.; Piotto, M.; Leppik, R.; Saudek, V. Gradient-Tailored Water Suppression for 1H-15N HSQC Experiments Optimized to Retain Full Sensitivity. *J. Magn. Reson. Series A* **1993**, *102*, 241−245.
(52) Fulton, D. B.; Hrabolr, N. F. Gradient Enhanced TOSCY Experiment with improved Sensitivity and Solvent Suppression, *J. Biomol. NMR* **1996**, 213−218.
(53) Trmble, L. A.; Bernstein, M. A. Application of Gradients for Water Suppression in 2D Multiple-Quantum-Filtered COSY spectra of peptides. *J. Magn. Reson. Ser. B*, **1994**, *105*, (1), 67−72.
(54) Sodano, P.; Delepierre, M. Clean and Efficient Suppression of the Water Signal in Multidimensional NMR Spectra. *J. Magn. Reson. Ser. A* **1993**, *104*, 88−92.
(55) Clore, G. M.; Brunger, A. T.; Karplus, M.; Gronenborn, A. M. Application of Molecular Dynamics with Interproton Distance Restraints to Three-dimensional Protein Structure Determination. A Model Study of Crambin. *J. Mol. Biol.* **1986**, *191*, 523−551.
(56) Wüthrich, K.; Billeter, M.; Braun, W. Pseudo-Structures for the 20 common Amino Acids for Use in Studies of Protein conformations by Measurements of Intramolecular Proton−Proton distance constraints with Nuclear magnetic Resonance. *J. Mol. Biol.* **1983**, *169*, 949−961.
(57) Sachais, B. S.; Snider, R. M.; Lowe, J. A. I.; Krause, J. E. Molecular basis for the species selectivity of the substance P antagonist CP-96,345. *J. Biol. Chem*. **1993**, *268*, 2319−2323.
(58) Blount, P.; Krause, J. E. Functional nonequivalence of structurally homologous domains of neurokinin-1 and neurokinin-2 type tachykinin receptors. *J. Biol. Chem*. **1993**, *268*, 16388−16395.
(59) Domann, R.; Martinez, J. Alternative to cloning cylinders for isolation of adherent cell clones. *Biotechniques* **1995**, *18*, 594−595.

JM000093V